

Rydberg Electrons in a Bose-Einstein Condensate

Jia Wang,¹ Marko Gacesa,¹ and Robin Côté¹

¹*Department of Physics, University of Connecticut, Storrs, CT 06269, USA*

We investigate a hybrid system composed of ultracold Rydberg atoms immersed in an atomic Bose-Einstein condensate (BEC). The coupling between the Rydberg electrons and BEC atoms leads to the excitation of phonons, the exchange of which induces Yukawa interaction between Rydberg atoms. Due to the small electron mass, the effective charge associated with this quasi-particle-mediated interaction can be large, while its range is equal to the healing length of the BEC, which can be tuned by adjusting the scattering length of the BEC atoms. We find that for small healing lengths, the distortion of the BEC can “image” the wave function density of the Rydberg electron, while large healing lengths induce an attractive Yukawa potential between the two Rydberg atoms that can form a new type of ultra-long-range molecule. We discuss both cases for a realistic system.

Impurities in a Bose-Einstein condensate (BEC) have attracted much attention and motivated the investigation of a wide range of phenomena. For example, the motion of a single impurity in a BEC can probe the superfluid dynamics [1–3], while an ionic impurity in a BEC can form a mesoscopic molecular ion [4]. Due to the self-energy induced by phonons (excitations of the BEC), a neutral impurity can self-localize in both a homogeneous and a harmonically trapped BEC [5–7], which sheds light on polaron physics [8, 9]. Exchanging phonons between multiple impurities induces an attractive Yukawa potential between each pair of impurities [10, 11], which leads to the so called “co-self-localization” [12] and is related to forming bipolarons and multipolarons [13]. Recent experiments, where an atom of a BEC is excited into a Rydberg state [14] to study phonon excitations and collective oscillations, open the door to exploration of the electron-phonon coupling in ultracold degenerate gases, a phenomenon responsible for the formation of Cooper pairs of two repelling electrons in BCS superconductivity [15].

In this Letter, we study Rydberg atoms immersed in a homogeneous BEC, as sketched in Fig. 1(a). Rydberg atoms consist of an ion core and a highly excited electron with its oscillatory wave function Ψ_e extending to large distances of the order of $\sim n^2 a_0$ (n : principle quantum number, a_0 : Bohr radius). As pointed out by Fermi [16], the interaction between the quasi-free electron at \mathbf{x} and a ground state atom at \mathbf{r} can be approximated at low scattering energies by a contact interaction parametrized by an energy-dependent s -wave scattering length $A_s(k) = -k^{-1} \tan \delta_s(k)$,

$$V_s(\mathbf{x}, \mathbf{r}) = \frac{2\pi\hbar^2}{m_e} A_s[k(r)] \delta^{(3)}(\mathbf{x} - \mathbf{r}). \quad (1)$$

While the s -wave approximation is valid for qualitative analysis, we include higher-partial wave contributions for quantitative results [17]. $A_s(k)$ depends on the scattering energy via the local wave number $k(r)$ given by

$$\frac{\hbar^2 k(r)^2}{2m_e} = -\frac{R_y}{(n - \delta_{\ell_e})^2} + \frac{e^2}{4\pi\epsilon_0 r}, \quad (2)$$

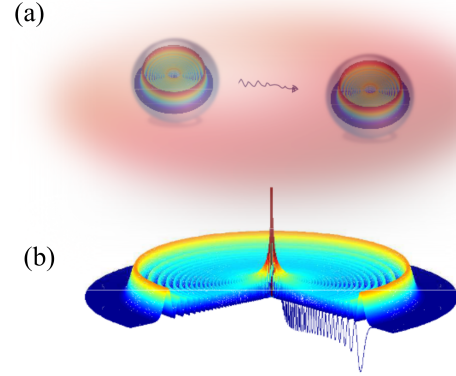


FIG. 1: (Color online) (a) Sketch: two Rydberg atoms immersed in an atomic BEC exchange phonons. The Rydberg electrons are represented by the surface plots inside the spheres, plotted in (b) along with the interaction potential curve within the s -wave approximation.

where R_y is the Rydberg constant, ϵ_0 the vacuum permittivity, e and m_e the charge and mass, respectively, of the electron with angular momentum ℓ_e and quantum defect δ_{ℓ_e} . For low- ℓ_e state, Eq.(1) gives an effective interaction between Rydberg and ground state atoms as

$$V_R(\mathbf{r}) \approx \frac{2\pi\hbar^2 A_s[k(r)]}{m_e} |\Psi_e(\mathbf{r})|^2, \quad (3)$$

which leads to an attraction and formation of ultra-long-range Rydberg molecules for $A_s < 0$ [18]. The electron density and corresponding oscillatory potential are sketched in Fig. 1(b) for a Rydberg ns ($\ell_e = 0$) state. High- ℓ_e states with negligible δ_{ℓ_e} are nearly degenerate, and their coupling gives electronic wave functions with strong quantum interference patterns. For alkali metals (*e.g.*, Rb or Cs), these interactions are strong enough to support very extended bound states, usually referred to as “trilobite states”, that possess a strong permanent dipole moment. The observation of “trilobite-like states”

[19–23], has motivated the studies of the p -wave electron (leading to “butterfly states” [24]), and Rydberg electrons scattering off a perturber with a permanent dipole moment [25].

In our system, Rydberg electrons interact with the coherent ground state of BEC, *i.e.* with many atoms, resulting in collective excitations described as phonons (scalar bosons). One of the most profound conceptual advances in physics is that the exchange of particles can produce a force (*e.g.*, the electromagnetic force is generated by charges exchanging virtual photons). Exchanging phonons in a BEC will lead to a Yukawa potential. As we describe below, under appropriate conditions, we find two regimes. For a BEC with a small healing length ξ , the Yukawa potential is short-ranged, and distorts the BEC locally, “mapping” the electron density onto the BEC density. For a large ξ , the Yukawa potential is long-ranged and can bind Rydberg atoms and form a new type of “ultra-long-range” molecule.

We first consider a homogeneous BEC in the absence of impurities, described by the Hamiltonian

$$H_{\text{BEC}} = \sum_{\mathbf{k}} \frac{\hbar^2 k^2}{2m_B} c_{\mathbf{k}}^\dagger c_{\mathbf{k}} + \frac{u_B}{2\Omega_V} \sum_{\mathbf{k}\mathbf{p}\mathbf{q}} c_{\mathbf{k}}^\dagger c_{\mathbf{p}}^\dagger c_{\mathbf{q}} c_{\mathbf{k}+\mathbf{p}-\mathbf{q}}, \quad (4)$$

where $u_B = 4\pi\hbar^2 a_B/m_B$ is the coupling constant between the atoms of mass m_B and scattering length a_B , Ω_V is the quantization volume, and $c_{\mathbf{k}}^\dagger$ ($c_{\mathbf{k}}$) is the creation (annihilation) operator of bosonic atoms with momentum \mathbf{k} . If most atoms occupy the ground state ($\mathbf{k}=0$), one can replace c_0^\dagger and c_0 by the c -number $\sqrt{N_0}$ and expand Eq.(4) in the decreasing order of N_0 . The number of atoms is given by $N = N_0 + \sum_{\mathbf{k} \neq 0} c_{\mathbf{k}}^\dagger c_{\mathbf{k}}$. By keeping the terms of the order $\sqrt{N_0}$ or higher, H_{BEC} can be diagonalized via the Bogoliubov transformation $c_{\mathbf{q}}^\dagger = u_{\mathbf{q}} b_{\mathbf{q}}^\dagger + v_{\mathbf{q}} b_{-\mathbf{q}}$. The resulting effective Hamiltonian is $\mathcal{H}_{\text{BEC}} = \sum_{\mathbf{q}} \hbar\omega_{\mathbf{q}} (b_{\mathbf{q}}^\dagger b_{\mathbf{q}} + 1/2)$, where $\hbar\omega_{\mathbf{q}} = (\epsilon_{\mathbf{q}}^2 + 2u_B \rho_B \epsilon_{\mathbf{q}})^{1/2}$, with $\epsilon_{\mathbf{q}} = \hbar^2 q^2/2m_B$ and the BEC number density $\rho_B = N/\Omega_V$. The Bogoliubov operator $b_{\mathbf{q}}^\dagger$ ($b_{\mathbf{q}}$) creates (annihilates) a quasi-particle (or phonon) of momentum \mathbf{q} when applied to the ground state $|0\rangle$: $b_{\mathbf{q}}^\dagger|0\rangle = |\mathbf{q}\rangle$. The local density operator $\hat{\rho}(\mathbf{r}) = \Omega_V^{-1} \sum_{\mathbf{p}, \mathbf{q}} e^{i\mathbf{q}\cdot\mathbf{r}} c_{\mathbf{p}+\mathbf{q}}^\dagger c_{\mathbf{p}}$ can be written as,

$$\hat{\rho}(\mathbf{r}) \approx \frac{N_0}{\Omega_V} + \frac{\sqrt{N_0}}{\Omega_V} \sum_{\mathbf{q} \neq 0} e^{i\mathbf{q}\cdot\mathbf{r}} (u_{\mathbf{q}} + v_{\mathbf{q}}) (b_{\mathbf{q}}^\dagger + b_{-\mathbf{q}}), \quad (5)$$

and the interaction between a Rydberg electron and BEC atoms $H_{\text{INT}} = \int d^3r \rho(\mathbf{r}) V_R(\mathbf{r})$ as

$$H_{\text{INT}} \approx \frac{N_0}{\Omega_V} V_0 + \frac{\sqrt{N_0}}{\Omega_V} \sum_{\mathbf{q} \neq 0} (u_{\mathbf{q}} + v_{\mathbf{q}}) (b_{\mathbf{q}}^\dagger + b_{-\mathbf{q}}) V_{\mathbf{q}}, \quad (6)$$

where $V_{\mathbf{q}} = \int d^3r V_R(\mathbf{r}) e^{i\mathbf{q}\cdot\mathbf{r}}$ is the Fourier transform of the potential. Applying the perturbation theory gives

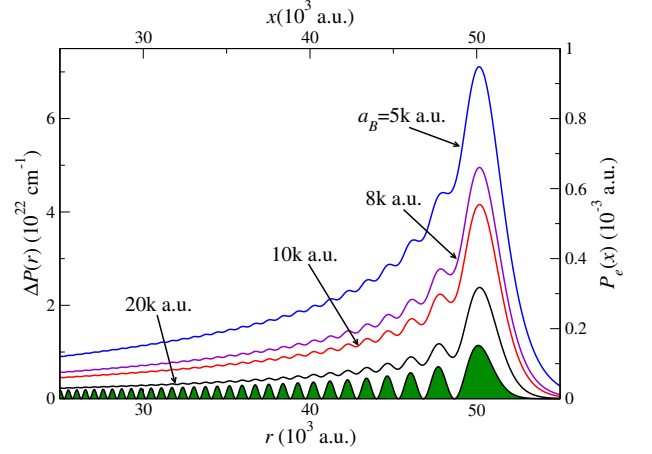


FIG. 2: (Color online) Comparison of radial electron probability density $P_e(x) = 4\pi x^2 |\Psi_e(x)|^2$ (green filled curve) and BEC local density distortion $\Delta P(r) = 4\pi r^2 \delta\rho(r)$ (solid curves) for a ^{87}Rb BEC with density $\rho_B = 2 \times 10^{13} \text{ cm}^{-3}$ and various scattering length a_B (in units of $k=10^3 a_0$) as indicated.

the first and second order corrections to the ground state energy: $E^{(1)} = \int d^3r \rho_B V_R(\mathbf{r})$ and

$$E^{(2)} = -\frac{\rho_B m_B}{2\pi\hbar^2} \int d^3r d^3r' V_R(\mathbf{r}) \frac{e^{-|\mathbf{r}-\mathbf{r}'|/\xi}}{|\mathbf{r}-\mathbf{r}'|} V_R(\mathbf{r}'), \quad (7)$$

by taking the thermal limit of $V^{-1} \sum_{\mathbf{q}} \rightarrow (2\pi)^{-3} \int d^3q$ and integrating over \mathbf{q} , where ρ_B is assumed to be a constant. Note that N_0 can be replaced by the total atom number N at this level of approximation.

Under approximation in Eq. (1), $E^{(1)} = 2\pi\rho_B \hbar^2 \bar{a}_e/m_e$ is the mean-field energy shift given in terms of the average scattering length $\bar{a}_e = \int d^3r A_s[k(r)] |\Psi_e(\mathbf{r})|^2$, while $E^{(2)} \approx \int d^3r d^3r' |\Psi_e(\mathbf{r})|^2 V_Y(\mathbf{r}-\mathbf{r}') |\Psi_e(\mathbf{r}')|^2/2$ involves the Yukawa potential

$$V_Y(\mathbf{r}-\mathbf{r}') = -\tilde{Q}^2 \frac{e^{-|\mathbf{r}-\mathbf{r}'|/\xi}}{|\mathbf{r}-\mathbf{r}'|}, \quad (8)$$

where its range $\xi = 1/\sqrt{16\pi\rho_B a_B}$ is exactly equal to the BEC healing length, and $\tilde{Q}^2 \approx 4\pi\hbar^2 \bar{a}_e^2 \rho_B m_B/m_e^2$ characterizes its strength; the “effective charge” \tilde{Q} emphasizes the analogy with Coulomb interactions. The term $E^{(2)}$ can be understood as the self-interaction of electrons by a Yukawa potential induced via phonon exchange at two different positions. This term is crucial in studies of self-localization of impurities in a BEC. However, in our system, the Rydberg electrons are already localized by strong Coulomb forces with ion cores. Therefore, the distorted BEC density, under appropriate conditions, can reflect the oscillatory nature of Ψ_e and “image” the Rydberg electron.

To the first order, the perturbed ground state given by $|\tilde{0}\rangle = |0\rangle - (\sqrt{N_0}/\Omega_V) \sum_{\mathbf{q} \neq 0} (u_{\mathbf{q}} + v_{\mathbf{q}}) V_{\mathbf{q}}/(\hbar\omega_{\mathbf{q}}) |\mathbf{q}\rangle$

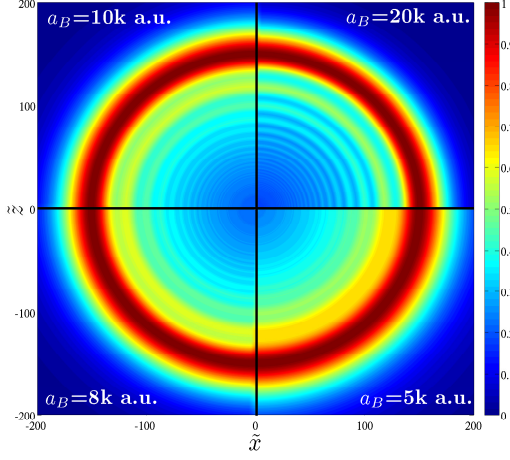


FIG. 3: (Color online) The BEC density distortion $\Delta P_{2D}/\max(\Delta P_{2D})$ in the x - z plane, where $\Delta P_{2D} = 2\pi r\delta\rho$. To better illustrate the oscillatory behavior at large distances, we use an exponential scale: $\tilde{x} = \exp(x/l_0)$ and $\tilde{z} = \exp(z/l_0)$, where $l_0 = 1\text{ k a.u.}$

leads to the BEC density distortion $\delta\rho(\mathbf{r}) \equiv \langle\hat{\rho}(\mathbf{r})\rangle - \rho_B$

$$\frac{\delta\rho(\mathbf{r})}{\rho_B} = -\frac{m_B}{\hbar^2\pi} \int d^3r' V_R(\mathbf{r}') \frac{e^{-|\mathbf{r}-\mathbf{r}'|/\xi}}{|\mathbf{r}-\mathbf{r}'|}. \quad (9)$$

Eq. (9) shows that $\delta\rho(\mathbf{r})$ is affected by “averaging” the effective interaction V_R within the range ξ . The oscillatory nature of Ψ_e can be imaged onto $\delta\rho(\mathbf{r})$ [26]. However, if ξ is larger than the local wavelength of the Rydberg electron, the averaging will erase this signature. This effect is illustrated in Fig. 2 for a $^{87}\text{Rb}(160\text{s})$ Rydberg atom in a ^{87}Rb BEC with $\rho_B = 2 \times 10^{13} \text{ cm}^{-3}$, by comparing the radial probability density $P_e(x) = 4\pi x^2 |\Psi_e(x)|^2$ with $\Delta P(r) = 4\pi r^2 \delta\rho(r)$ for different scattering lengths a_B . Larger values of a_B produce a sharper signature of the oscillation, albeit an overall smaller distortion amplitude. This effect is better illustrated in a 2D density plot (Fig. 3), where different quadrants represent the “normalized” 2D distortion densities $\Delta P_{2D}/\max(\Delta P_{2D})$ in the x - z plane for four different a_B . Here, $\Delta P_{2D} = 2\pi r\delta\rho$, and x and z are rescaled by $\tilde{x} = \exp(x/l_0)$ and $\tilde{z} = \exp(z/l_0)$, where $l_0 = 1\text{ k a.u.}$, so that the effects at large distances are emphasized. It is evident that the oscillations for $a_B = 5\text{ k a.u.}$ (fourth quadrant) are much blurrier than for $a_B = 20\text{ k a.u.}$ (first quadrant).

For a large healing length ξ , the averaging of V_R masks the effect of the electron self-interaction due to the phonon exchange. However, the phonon exchange still mediates non-trivial interactions between the Rydberg atoms. Without a BEC, two Rydberg atoms experience strong long-range interactions, leading to formation of macrodimers [27] and the interaction blockade [28–32]. For two ns Rydberg atoms separated by R , this interaction is repulsive with its leading term being the

van-der-Waals (vdW) $+C_6/R^6$ term, where $C_6 \propto n^{11}$ [33]. Immersed in a BEC, however, the exchange of phonons between two Rydberg atoms gives rise to a Yukawa potential. We derive this potential within the Born-Oppenheimer (BO) approximation, starting from the interaction of two Rydberg atoms, located at \mathbf{R}_1 and \mathbf{R}_2 , and BEC atoms (after applying the Bogoliubov transformation)

$$H_{\text{INT}} \approx \frac{N_0}{\Omega_V} {}^1\mathcal{V}_0 + \frac{N_0}{\Omega_V} {}^2\mathcal{V}_0 + \frac{\sqrt{N_0}}{\Omega_V} \sum_{\mathbf{q} \neq 0} (u_{\mathbf{q}} + v_{\mathbf{q}}) \times (b_{\mathbf{q}}^\dagger + b_{-\mathbf{q}}) ({}^1\mathcal{V}_{\mathbf{q}} e^{i\mathbf{q}\cdot\mathbf{R}_1} + {}^2\mathcal{V}_{\mathbf{q}} e^{i\mathbf{q}\cdot\mathbf{R}_2}). \quad (10)$$

Here, ${}^i\mathcal{V}_{\mathbf{q}} \equiv \int d^3r V_i(\mathbf{r}) e^{i\mathbf{q}\cdot\mathbf{r}}$, where $V_i(\mathbf{r})$ describes the interaction of “impurity” i and the BEC atoms in coordinate space. Within perturbation theory, the first order correction $E^{(1)}$ gives a mean-field energy shift similar to the single Rydberg atom case in the thermal limit. For spherically symmetric interactions (where ${}^i\mathcal{V}_{\mathbf{q}} = {}^i\mathcal{V}_{-\mathbf{q}}$ is real), the second order correction is

$$E^{(2)} = -\frac{\rho_B}{(2\pi)^3} \int d^3q \frac{A_q + 2B_q e^{iqR \cos \theta_q}}{\epsilon_q + 2u_B \rho_B}, \quad (11)$$

where $A_q = ({}^1\mathcal{V}_q)^2 + ({}^2\mathcal{V}_q)^2$, $B_q = {}^1\mathcal{V}_q \cdot {}^2\mathcal{V}_q$, $R = |\mathbf{R}_1 - \mathbf{R}_2|$ is the Rydberg atoms separation, and θ_q is the angle between the vector \mathbf{R} and \mathbf{q} . The term containing A_q can be understood as the self-localizing energy for both Rydberg atoms calculated previously, and will be neglected together with the mean-field energy shift $E^{(1)}$ for the study of relative dynamics of Rydberg atoms, since they simply contribute a constant energy shift. The term containing B_q leads to the BO potential

$$U(R) = -\frac{\rho_B}{(2\pi)^3} \int d^3q \frac{2B_q e^{iqR \cos \theta_q}}{\epsilon_q + 2u_B \rho_B}, \quad (12)$$

which can be easily generalized to interactions between any two impurities immersed in a BEC [11].

The BO approach allows the study of the adiabatic corrections induced by the motion of Rydberg atoms. The diagonal adiabatic correction $\Delta E^{(2)} = \hbar^2 \langle \tilde{0} | \tilde{\partial}_R \tilde{\partial}_R | \tilde{0} \rangle / m_I$ depends on the impurity mass m_I , where $|\tilde{0}\rangle = |0\rangle - \sum_{\mathbf{q} \neq 0} \frac{\langle \mathbf{q} | H_{\text{INT}} | 0 \rangle}{\hbar \omega_q} |\mathbf{q}\rangle$ is the perturbed ground state. Therefore, $\Delta E^{(2)} = \frac{\hbar^2}{m_I} \sum_{\mathbf{q} \neq 0} \frac{\langle 0 | \partial_R H_{\text{INT}} | \mathbf{q} \rangle \langle \mathbf{q} | \partial_R H_{\text{INT}} | 0 \rangle}{\hbar^2 \omega_q^2}$, so that, in the thermal limit and neglecting the constant energy shift terms, the diabatic correction to $U(R)$ is

$$\Delta U(R) = -\frac{\hbar^2}{2m_I} \frac{\rho_B}{(2\pi)^3} \int d^3q \frac{B_q q^2 \cos^2 \theta_q e^{iqR \cos \theta_q}}{\sqrt{\epsilon_q(\epsilon_q + 2u_B \rho_B)^3}}. \quad (13)$$

The $e^{iqR \cos \theta_q}$ term in Eqs. (12) and (13) implies that, for a large R , only the terms where q is small are important, leading to the asymptotic behavior of the potential $U(R) \rightarrow -\tilde{Q}^2 e^{-R/\xi}/R$, where $\tilde{Q}^2 \approx$

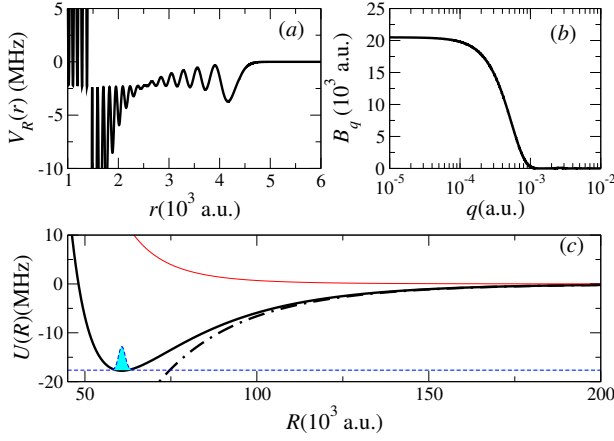


FIG. 4: (Color online) (a) Interaction potential between a Rydberg $^{87}\text{Rb}(50s)$ atom and a ground state ^{87}Rb atom. (b) B_q as a function of q . (c) Effective potential between two Rydberg $^{87}\text{Rb}(50s)$ atoms in a BEC. The tail is dominated by the Yukawa potential (dash-dotted curve) while the blue filled curve represents the lowest bound state.

$\rho_B m_B B_{q=0}/\pi$. For the s -wave, the effective charge is $\tilde{Q}^2 \approx 4\pi\hbar^2 \tilde{a}_e^2 \rho_B m_B / m_e^2$. Not surprisingly, we obtain the same Yukawa potential as in Eq. (8), since phonon-exchange mediates the interaction. Note that \tilde{Q} is inversely proportional to m_e for Rydberg atoms, since the electrons are really the perturbors, as opposed to more massive neutral impurities for which \tilde{Q} is inversely proportional to m_I . Hence, the induced interaction is much stronger for Rydberg atoms. Under the same approximation, the adiabatic correction is given by $\Delta U(R) \rightarrow (m_B/m_I)(\tilde{Q}^2/2\xi)F(R/\xi)$, with $F(x)$ defined as $F(x) = \frac{2}{\pi} - \frac{4}{\pi x^2} - \frac{2f(-1,x)}{x^2} + \frac{f(0,x)}{x} - f(1,x)$, where $f(n,x) = I_n(x) - L_n(x)$ is given in terms of the modified Bessel function of the first kind $I_n(x)$ and the modified Struve function $L_n(x)$. The asymptotic behaviors are $F(R/\xi) \rightarrow 4/(3\pi)$ for $R \ll \xi$, and $F(R/\xi) \rightarrow 12\xi^4/(\pi R^4)$ for $R \gg \xi$. We note that for $R \gg \xi$, these imply a vanishing adiabatic potential $U(R)$ so that the adiabatic correction becomes dominated by a repulsive $1/R^4$ term. As expected, the diabatic correction can be neglected if $m_B \ll m_I$. A surprising limit is reached for a very large healing length ξ , which can be achieved by using a Feshbach resonance to tune $a_B \rightarrow 0$. Then, the diabatic correction also vanishes: $\lim_{\xi \rightarrow \infty} \Delta U(R) = 0$, even when m_B is larger than m_I . Notice that, in this limit, $U(R)$ reduces to the Coulomb potential.

To illustrate these predictions, we consider a realistic system of two $^{87}\text{Rb}(50s)$ Rydberg atoms immersed in a BEC of ^{87}Rb atoms of density $\rho_B = 10^{13} \text{ cm}^{-3}$. To ensure a healing length ξ much larger than the Rydberg atoms, the scattering length between the BEC atoms is tuned to $a_B = 10 \text{ a.u.}$ (e.g., via a Feshbach resonance), so that $\xi = 3.66 \times 10^4 \text{ a.u.}$ The numerical “trilobite-like” interaction shown in Fig. 4(a) is constructed us-

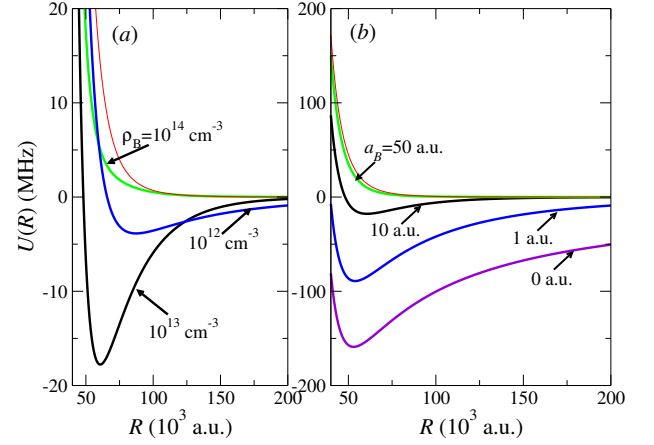


FIG. 5: (Color online) The thin solid red curves show the dispersion interactions between two $^{87}\text{Rb}(50s)$ atoms in a vacuum, while the thick curves show the interaction between these two Rydberg atoms immersed in a BEC with (a) fixed $a_B = 10 \text{ a.u.}$ but different density ρ_B and (b) fixed $\rho_B = 10^{13} \text{ cm}^{-3}$ but different scattering length a_B .

ing the first-order perturbative model [16, 34] including s - and p - contributions [17], with zero-energy scattering lengths, $A_s = -16.05 a_0$ and $A_p = -21.15 a_0$, respectively [35]. The states in the range $n = 47 - 51$ were included and the resulting Hamiltonian diagonalized to obtain the $50s$ eigenstate [36]. Fig. 4(b) shows that B_q computed using this potential converges to a constant $B_{q=0} \approx 2 \times 10^4 \text{ a.u.}$ for a small q , yielding an effective charge $\tilde{Q}^2 \approx 1.537 \times 10^{-3} \text{ a.u.}$ Fig. 4(c) depicts the effect of immersing Rydberg atoms in a BEC: without the BEC, two Rydberg atoms interact via the vdW potential $-C_6/R^6 - C_8/R^8 - C_{10}/R^{10}$ (repulsive solid-red curve with $C_6 = -1.074 \times 10^{20}$, $C_8 = 7.189 \times 10^{26}$, and $C_{10} = -7.162 \times 10^{33}$, in a.u. for $^{87}\text{Rb}(50s)$ [37].) In a BEC, the BO potential (solid black curve) is attractive at large separations, in agreement with the Yukawa potential $-\tilde{Q}^2 e^{-R/\xi}/R$ (dash-dotted curve) at large distances, before becoming repulsive at shorter range where the “bare” repulsive vdW interaction dominates the phonon-exchange contribution. The well produced by the phonon-exchange can support bound levels; in the example above, its depth is about -17.77 MHz , while the equilibrium separation is about $60k \text{ a.u.}$ (much larger than the $5k \text{ a.u.}$ extension of the “trilobite-like” potentials). The large mass of Rb atoms leads to many bound levels; the three lowest are at about -17.64 MHz , -17.56 MHz and -17.47 MHz . The ground state wave function with a spatial width about $2k \text{ a.u.}$ is also shown in Fig. 4(c),

These results show how phonon-exchange modifies an otherwise repulsive interaction into a potential well capable of binding two Rydberg atoms. Fig. 5 explores the sensitivity of the BO potentials to variations in density ρ_B and scattering length a_B , and compares them to the “bare” case (without BEC). The behavior of the BO

curves can be understood qualitatively from the s -wave approximation with average scattering length \bar{a}_e : \tilde{Q}^2 is proportional to ρ_B and ξ to $\rho_B^{-1/2}$. The competition between the two effects as ρ_B varies leads to a deeper BO curve for a moderate density (see Fig. 5(a)). However, \tilde{Q}^2 is independent of a_B while ξ is proportional to $a_B^{-1/2}$, giving deeper BO curves as a_B gets smaller (see Fig. 5(a)). Hence, the BEC-induced interaction can be conveniently controlled by tuning a_B via a Feshbach resonance; in the limit $a_B = 0$, the long-range Yukawa potential becomes an attractive Coulomb potential.

In summary, we studied BEC-induced interactions involving Rydberg impurities due to phonon-exchange, and found two limiting cases depending on the healing length ξ of the BEC. For a small ξ , the BEC modulation can be used to “image” the wave function of the Rydberg electron, while large ξ leads to the formation of ultra-long-range diatomic molecules. By tuning a_B , “synthetic” Coulomb potentials can be generated between neutral particles and their sign can be modified by using different Rydberg states for the two impurity atoms. This long range interaction is well-behaved and easily controlled and, hence, opens promising avenues of research. For example, for systems containing many Rydberg atoms impurities, this interaction might lead to crystallization [38], and be used to study the phase diagram of Yukawa bosons [39].

This work was partially supported by the U.S. Department of Energy, Office of Basic Energy Sciences (J.W.), the Army Research Office Grant No. W911NF-13-1-0213 (M.G.), and the National Science Foundation Grant No. PHY 1101254 (R.C.)

[1] E. Timmermans and R. Côté, Phys. Rev. Lett. **80**, 3419 (1998).
[2] A. P. Chikkatur, A. Görlitz, D. M. Stamper-Kurn, S. Inouye, S. Gupta, and W. Ketterle, Phys. Rev. Lett. **85**, 483 (2000).
[3] G. E. Astrakharchik and L. P. Pitaevskii, Phys. Rev. A **70**, 013608 (2004).
[4] R. Côté, V. Kharchenko, and M. D. Lukin, Phys. Rev. Lett. **89**, 093001 (2002).
[5] K. Sacha and E. Timmermans, Phys. Rev. A **73**, 063604 (2006).
[6] R. M. Kalas and D. Blume, Phys. Rev. A **73**, 043608 (2006).
[7] M. Bruderer, W. Bao, and D. Jaksch, Europhys. Lett. **82** (2008).
[8] F. M. Cucchietti and E. Timmermans, Phys. Rev. Lett. **96**, 210401 (2006).
[9] A. A. Blinova, M. G. Boshier, and E. Timmermans, Phys. Rev. A **88**, 053610 (2013).
[10] L. Viverit, C. J. Pethick, and H. Smith, Phys. Rev. A **61**, 053605 (2000).
[11] M. J. Bijlsma, B. A. Heringa, and H. T. C. Stoof, Phys. Rev. A **61**, 053601 (2000).

[12] D. H. Santamore and E. Timmermans, New J. Phys. **13** (2011).
[13] W. Casteels, J. Tempere, and J. T. Devreese, Phys. Rev. A **88**, 013613 (2013).
[14] J. B. Balewski, A. T. Krupp, A. Gaj, D. Peter, H. P. Büchler, R. Löw, S. Hofferberth, and T. Pfau, Nature (London) **502**, 664 (2013).
[15] J. Bardeen, L. N. Cooper, and J. R. Schrieffer, Phys. Rev. **108**, 1175 (1957).
[16] E. Fermi, Il Nuovo Cimento **11**, 157 (1934), ISSN 1827-6121.
[17] $V_p(\mathbf{x}, \mathbf{r}) = (6\pi\hbar^2/m_e)A_p^3(k)\delta^{(3)}(\mathbf{x} - \mathbf{r}) \overleftarrow{\nabla} \cdot \overrightarrow{\nabla}$ for p -wave, with $k^3 A_p^3(k) = -\tan \delta_p(k)$.
[18] C. H. Greene, A. S. Dickinson, and H. R. Sadeghpour, Phys. Rev. Lett. **85**, 2458 (2000).
[19] V. Bendkowsky, B. Butscher, J. Nipper, J. P. Shaffer, R. Löw, and T. Pfau, Nature (London) **458**, 1005 (2009).
[20] W. Li, T. Pohl, J. M. Rost, S. T. Rittenhouse, H. R. Sadeghpour, J. Nipper, B. Butscher, J. B. Balewski, V. Bendkowsky, R. Löw, et al., Science **334**, 1110 (2011).
[21] M. A. Bellos, R. Carollo, J. Banerjee, E. E. Eyler, P. L. Gould, and W. C. Stwalley, Phys. Rev. Lett. **111**, 053001 (2013).
[22] A. Krupp, A. Gaj, J. Balewski, P. Ilzhöfer, S. Hofferberth, R. Löw, T. Pfau, M. Kurz, and P. Schmelcher, arXiv: 1401.2477v1 (2014).
[23] D. A. Anderson, S. A. Miller, and G. Raithel, arXiv: 1401.2477v1 (2014).
[24] E. L. Hamilton, C. H. Greene, and H. R. Sadeghpour, J. Phys. B: At. Mol. Opt. Phys. **35**, L199 (2002).
[25] M. Mayle, S. T. Rittenhouse, P. Schmelcher, and H. R. Sadeghpour, Phys. Rev. A **85**, 052511 (2012).
[26] T. Karpiuk, M. Brewczyk, K. Rzażewski, J. B. Balewski, A. T. Krupp, A. Gaj, R. Löw, S. Hofferberth, and T. Pfau, arXiv:1402.6875 (2014).
[27] C. Boisseau, I. Simbotin, and R. Côté, Phys. Rev. Lett. **88**, 133004 (2002).
[28] M. D. Lukin, M. Fleischhauer, R. Cote, L. M. Duan, D. Jaksch, J. I. Cirac, and P. Zoller, Phys. Rev. Lett. **87**, 037901 (2001).
[29] D. Tong, S. M. Farooqi, J. Stanojevic, S. Krishnan, Y. P. Zhang, R. Côté, E. E. Eyler, and P. L. Gould, Phys. Rev. Lett. **93**, 063001 (2004).
[30] K. Singer, M. Reetz-Lamour, T. Amthor, L. G. Marcassa, and M. Weidemüller, Phys. Rev. Lett. **93**, 163001 (2004).
[31] T. Vogt, M. Viteau, J. Zhao, A. Chotia, D. Comparat, and P. Pillet, Phys. Rev. Lett. **97**, 083003 (2006).
[32] T. C. Liebisch, A. Reinhard, P. R. Berman, and G. Raithel, Phys. Rev. Lett. **95**, 253002 (2005).
[33] K. R. Overstreet, A. Schwettmann, J. Tallant, D. Booth, and J. P. Shaffer, Nature Phys. **5**, 581 (2009).
[34] A. Omont, J. Phys. (Paris) **38**, 1343 (1977).
[35] V. Bendkowsky, B. Butscher, J. Nipper, J. B. Balewski, J. P. Shaffer, R. Löw, T. Pfau, W. Li, J. Stanojevic, T. Pohl, et al., Phys. Rev. Lett. **105**, 163201 (2010).
[36] This approach is expected to be valid for isolated ns Rydberg states considered here [24].
[37] K. Singer, J. Stanojevic, M. Weidemüller, and R. Côté, J. Phys. B: At. Mol. Opt. Phys. **38**, S295 (2005).
[38] D. C. Roberts and S. Rica, Phys. Rev. Lett. **102**, 025301 (2009).
[39] O. N. Osychenko, G. E. Astrakharchik, F. Mazzanti, and J. Boronat, Phys. Rev. A **85**, 063604 (2012).